X-Ray Diffraction Study of Lipid Bilayer Membranes Interacting with Amphiphilic Helical Peptides: Diphytanoyl Phosphatidylcholine with Alamethicin at Low Concentrations

Yili Wu, Ke He, Steve J. Ludtke, and Huey W. Huang
Physics Department, Rice University, Houston, Texas 77251-1892 USA

ABSTRACT A variety of amphiphilic helical peptides have been shown to exhibit a transition from adsorbing parallel to a membrane surface at low concentrations to inserting perpendicularly into the membrane at high concentrations. Furthermore, this transition has been correlated to the peptides' cytolytic activities. X-ray lamellar diffraction of diphytanoyl phosphatidylcholine-alamethicin mixtures revealed the changes of the bilayer structure with alamethicin concentration. In particular, the bilayer thickness decreases with increasing peptide concentration in proportion to the peptide-lipid molar ratio from as low as 1:150 to 1:47; the latter is near the threshold of the critical concentration for insertion. From the decreases of the bilayer thickness, one can calculate the cross sectional expansions of the lipid chains. For all of the peptide concentrations studied, the area expansion of the chain region for each adsorbed peptide is a constant 280 ± 20 Å^2, which is approximately the cross sectional area of an adsorbed alamethicin. This implies that the peptide is adsorbed at the interface of the hydrocarbon region, separating the lipid headgroups laterally. Interestingly, the chain disorder caused by a peptide adsorption tends to spread over a large area, as much as 100 Å in diameter. The theoretical basis of the long range nature of bilayer deformation is discussed.

INTRODUCTION

It is energetically favorable for amphiphilic helical peptides to adsorb on a membrane surface. If their lengths are about 30–40 Å, it may also be favorable for them to penetrate and traverse the hydrocarbon region of a lipid bilayer in some form of aggregate. For this reason, it is a common practice to identify such peptide segments as membrane-active (Kaiser and Kézdy, 1987; Segrest et al., 1990). In nature, membrane-active peptides appear either as a part of a complex protein or in free form. Perhaps the best known example of the former is the fusion peptides of viral fusion proteins (White, 1992). However, how the fusion peptides actually interact with a membrane is not known. Small, amphiphilic helix-forming peptides are produced by fungi as well as animals. Examples are: alamethicin, suzukacillin, and trichotoxin from fungi (Latorre and Alvarez, 1981); magainins (Zasloff, 1987), bombinin, and bambinin-like peptides (Gibson et al., 1991) from amphibians; melittins from bees (Habermann, 1972); cecropins from moths (Steiner et al., 1981); and cecropin P1 from pigs (Lee et al., 1989). These peptides are characterized by their tendency to form amphiphilic helices when associated with a membrane. Their primary functions are to rupture the membranes, which causes cytolysis. (In very low concentrations, they also form discrete ion channels and affect the cellular potentials, but whether that is the intended function is not known.) Indeed, all of them are known as antibiotics or antimicrobials, except for melittin, which is a hemolytic toxin. Because of their structural simplicity, they are ideal for the study of peptide-membrane interactions.

These peptides and their synthetic analogs have been shown to have common characteristics as well as differences in their interactions with lipid bilayer membranes (Huang and Wu, 1991; Ludtke et al., 1994). The common characteristics are that the peptides associate with a membrane in two ways. At low concentrations, the majority of them adsorbs parallel to the membrane surface; occasionally, by thermal fluctuations, some insert into the bilayer and form ion channels. At high concentrations, they insert perpendicularly in the bilayer. The transition between these two states occurs over a small range of concentration, indicating that it is a cooperative phenomenon, like a phase transition. In cells, such a peptide insertion transition would cause cytolysis, and that is the biological function of those peptides produced in the host defense systems of animals (Ludtke et al., 1994). The differences between different peptides include varying degrees of affinity toward a lipid bilayer and different critical concentrations for the insertion transition.

To understand the structural basis of the peptide-lipid interactions, we performed x-ray lamellar diffraction of lipid bilayers containing peptides at various concentrations. In most cases, the electron-density contrast between the peptide and lipid molecules and the weight fraction of the peptide relative to the lipid are both small, so that we cannot detect the peptide molecules directly. (The exceptional cases are the in-plane scattering at high concentrations of peptide where the helix packing produces a distinct scattering peak (publication in preparation).) What we have observed are the changes of the bilayer structure with the peptide concentration. In this first of a series of studies, we report the result on diphytanoyl phosphatidylcholine (DPhPC) interacting with alamethicin below the critical concentration for insertion. Alamethicin begins to insert into the DPhPC bilayer at

Received for publication 18 July 1994 and in final form 14 November 1994.
Address reprint requests to Dr. Huey W. Huang, Department of Physics, Rice University, Houston, TX 77251-1892. Tel.: 713-527-4899; Fax: 713-527-9033; E-mail: huang@ion.rice.edu.

0006-3495/95/06/2361/09 $2.00

a peptide/lipid molar ratio (P/L) ≈1:40 and is completely inserted at 1:15 (see Results and Discussion for differences with previously published results in Huang and Wu, 1991). The property of the membrane changes drastically when the peptide is inserted. Therefore, a separate report on the high concentration measurement is appropriate.

We found that when the peptides are adsorbed on the membrane surface, the lipid chains become disordered and the bilayer thickness decreases. The decrease of the bilayer thickness is proportional to the peptide concentration from P/L as low as 1:150 to 1:47, near the threshold of the critical concentration for insertion. Because the chain volume is approximately constant, the chain cross section must increase correspondingly, and from this one can calculate the area occupied by the adsorbed peptides. These results reveal a very simple way that alamethicin interacts with a DPhPC bilayer at low concentrations that leads to peptide insertion at high concentrations.

MATERIALS AND METHODS

Samples

1,2-diphytanoyl-*sn*-glycero-3-phosphatidylcholine in $CHCl_3$ was purchased from Avanti Polar Lipids (Alabaster, AL). Alamethicin was purchased from Sigma Chemical Co. (St. Louis, MO). Alamethicin was shown to be a mixture of components, principally alamethicins I (85% by HPLC) and alamethicin II (12%), which differ by one amino acid (Pandey et al., 1977). Both lipid and peptide were used without further purification. The sample preparation procedure followed that of Huang and Wu (1991). In brief, alamethicin and lipid at the desired peptide/lipid molar ratio (P/L) were first co-dissolved in chloroform/methanol. The solvent was removed by a slow nitrogen purge followed by drying under vacuum (10 μm) for at least 4 h. Distilled water was added to the peptide/lipid film. The mixture was homogenized with a tissue grinder and/or a sonicator so as to break up large aggregates. The lipid/peptide dispersion was lyophilized. The lyophilized powder was then hydrated with water vapor. A small amount from each sample batch was then sandwiched between two fused silica plates for oriented circular dichroism (OCD) measurement, or between one glass plate and one polished Be plate (Olah et al., 1991) for x-ray measurement. The thicknesses of the OCD samples are ~1 μm, and those of the x-ray samples are ~10 μm. Each sample was aligned homeotropically (lipid bilayers parallel to the substrate surfaces), and the alignment was examined by polarized microscopy as described in Huang and Olah (1987). All measurements were done at room temperature (25 ± 1°C).

Hydration of the samples

The water content of a multilayer sample was controlled by letting the sample come to equilibrium with air of a definite relative humidity. Two methods of humidity control were used in this experiment: a series of humidity chambers containing saturated solutions of various salts (O'Brien, 1948; Huang and Wu, 1991), and an air flow system with part of the air bubbling through a water tank. The second method was necessary because the first method allows only discrete values of relative humidity. Our goal was to vary the lamellar spacing D (i.e., the repeat distance) of the multilayers continuously. D can be measured from the positions of the Bragg peaks to at least three significant figures. Also, any significant inhomogeneity in the sample (in the degree of hydration or molecular distribution) will show up in the broadening of the diffraction peaks or even the appearance of double-peak patterns. Quantifying the correlation between the humidity and the lamellar spacing was difficult, particularly near 100% relative humidity, because of the lack of active temperature control.

OCD

Circular dichroism (CD) spectra were measured on a spectropolarimeter (JASCO J-500A, Japan). A small amount of alamethicin-lipid mixture was taken from each sample batch to prepare a vesicle suspension. Vesicular CD was measured following the procedure described in Wu et al. (1990). All samples showed the same vesicular CD representing the secondary structure of α helices (Chang et al., 1978; Wu et al., 1990). To determine the orientation of the helices with respect to the plane of the bilayer, we used the method of OCD described in Wu et al. (1990). This method makes use of the Moffitt theory (Moffitt, 1956) that the peptide's exciton band at 208 nm is polarized parallel to the helical axis (Olah and Huang, 1988). Thus, a normal incident CD of a multilayer sample shows, for helices parallel to the membranes, a 208-nm amplitude slightly larger than the corresponding vesicular CD, whereas the band disappears if the helices are perpendicular to the membranes (Wu et al., 1990). This simple method allowed us to examine the peptide orientation in a matter of minutes using a standard CD spectropolarimeter.

X-ray diffraction

Because our samples are virtually single-domain (smectic liquid) crystals, we used the ω-2θ scanning method to measure their diffraction patterns. This method provides a well defined diffraction geometry and, therefore, a precise reduction procedure for data analysis (Olah et al., 1991; Huang et al., 1991). The measurements were performed on a Huber 4-circle diffractometer with a line-focused (10 mm vertical × 1 mm horizontal) Cu K_α (λ = 1.54 Å) source operating at 40 kV and 15–30 mA; the current was adjusted to keep the intensity of the first Bragg peak from exceeding the maximum count rate of the detector (~4×10^4 s^{-1}). At a 6° take-off angle (the projected source dimension 10 × 0.1 mm^2), the incident beam was collimated by a horizontal soller slit and two vertical slits on the front and the rear sides of the soller slit. The horizontal and vertical divergence of the incident beam were 0.23° and 0.4°, respectively. The diffracted beam first passed through a vertical slit and then was discriminated by a bent graphite monochromator before entering a scintillation detector that was biased to discriminate against higher harmonics. A diffracted beam monochromator has the advantage over an incident beam monochromator in that the Compton scattering and the fluorescence from the sample are screened; consequently, the background signal is greatly reduced.

It is important to position and orient the multilayer sample correctly. After the incident beam was centered at $\theta = 0°$, the sample was mounted on the goniometer head with the planes of the multilayers in the x-y plane (where x denotes the direction of the incident beam $\theta = 0°$, and y the vertical). The absorption profiles of the Be plate and the glass plate are distinguishable. The z-position of the sample was adjusted so that the interface of glass and Be was at $\theta = 0°$. The zero point of ω was at this point roughly determined by a ω scan with θ fixed at 0°. The fine adjustment ω-zero was done as follows.

The alignment of the lipid multilayers was first examined qualitatively from the glass side by using a reflection-polarized microscope (Huang and Olah, 1987). It was then examined by an ω-θ two-dimensional scan around a Bragg peak. Because the two substrate surfaces usually are not exactly parallel to each other, the ω-θ two-dimensional scan usually shows two peaks, implying that there are two domains of smectic multilayers, one associated with each substrate surface. Usually one peak is much more pronounced than the other. We chose the dominant peak as the diffraction plane. At the center of the dominant peak, ω was set equal to $\theta/2$. The mosaic spread, defined as FWHM of the peak on the ω axis, was typically 0.2–0.3°.

The ω-2θ scan was repeated approximately every 1 h from $\omega = 0°$ to 10°, with the step size $\Delta\omega = 0.02°$, covering 10 Bragg orders. The sample was considered to be in equilibrium when five consecutive diffraction patterns remained unchanged within a few percent. The five scans were then averaged to create one diffraction pattern for analysis. Usually it took about 10 h for a sample to come to equilibrium for each D. Some typical scans of pure DPhPC are shown in Fig. 1.

All diffraction patterns included in this study (to be discussed in Fig. 6 below) consist of six or seven (mostly seven) discernible Bragg peaks (e.g.,

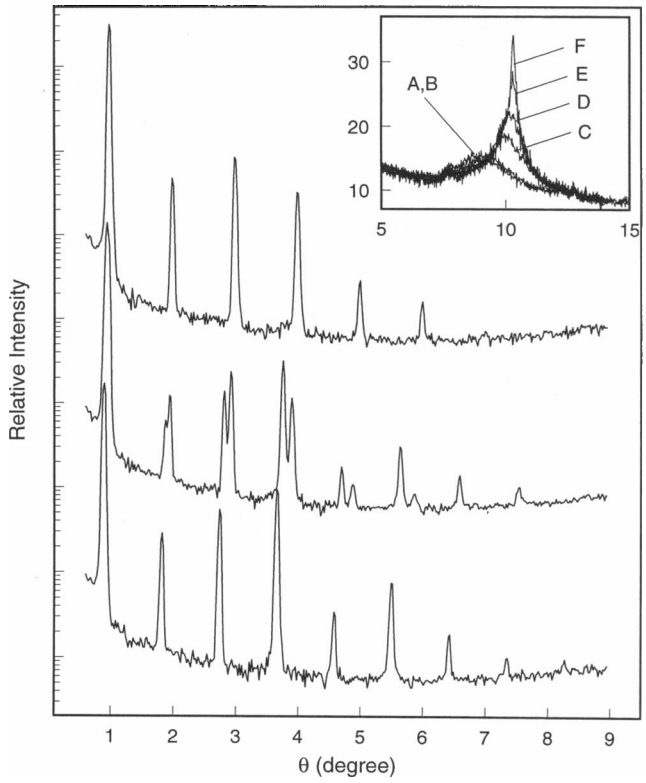

FIGURE 1 Typical diffraction patterns of pure DPhPC multilayers in wet (*bottom*, D = 48.3 Å) and dry (*top*, D = 44.4 Å) conditions. The middle diffraction pattern shows equilibrium coexistence of two phases (D = 45.4 and 47.1 Å). The inset shows the in-plane scattering (He et al., 1993) of the chain packing, the so-called wide-angle bands: DPhPC has a diffuse band at ~9°. The band is independent of the hydration condition (*A*, wet; *B*, dry, one on the top of the other) and independent of the presence of alamethicin (not shown). In comparison, dilauroyl phosphatidylcholine (DLPC), at the same temperature (25 ± 1°C), has a better defined band at ~10° in wet condition (*C*) representing the L_α phase; the band progressively sharpens (*D–F*) as the multilayers were dried and changed to the gel phase (data taken from He et al., 1993).

Fig. 1, *top*). The exceptions are pure DPhPC in the wet conditions where eight, or sometimes nine, peaks are discernible (e.g., Fig. 1, *bottom*). The quality of the diffraction patterns will be discussed below.

The procedure for data reduction has been described previously (Olah et al., 1991; Huang et al., 1991). After background subtraction, the diffraction intensity is corrected first for absorption and diffraction volume. These corrections (particularly for the first few Bragg orders) are sensitive to the beam geometry, so they were calculated by constructing a ray diagram. At each θ, the incident beam was divided into 300 sub-rays. The absorption and diffraction volume of each sub-ray was calculated separately. The rest of the data reduction is not very sensitive to small variations of θ, so the intensity was integrated for each Bragg peak after the absorption and diffraction volume corrections. The integrated intensity was then corrected for the polarization and the Lorentz factors. Thus, we obtained the relative magnitude of the scattering amplitude $|F(q)| = |F(2\pi h/D)|$ for the diffraction pattern of lamellar spacing D, Bragg order h, where q is the magnitude of the x-ray momentum transfer $4\pi\sin\theta/\lambda$.

We note that there was one more possible correction to be considered. If the incident x-ray beam has an angular divergence and the sample is mosaic, the vertical size of the Bragg reflections will increase with order. In the vertical direction, the slit width may be smaller than the width of the Bragg reflection; therefore, a correction factor has to be introduced that accounts for the increasing loss in intensity with order (Saxena and Schoenborn, 1977). This correction factor for our experiment turned out to be negligible, less than 0.1% for the eighth order. In other words, our vertical opening was sufficiently wide that the detector practically intercepted the whole Bragg reflection for every order.

The phases of the scattering amplitudes were determined by the well known swelling method (e.g., Blaurock, 1971; Torbet and Wilkins, 1976; Olah et al., 1991). For each diffraction pattern, an overall factor was multiplied to all scattering amplitudes to satisfy Blaurock's scaling relation (Blaurock, 1971):

$$\sum_h \left|F\left(\frac{2\pi h}{D}\right)\right|^2 = \frac{D}{D_o}$$

where D_0 is a constant (an arbitrarily chosen value of D) for the swelling series. The scaled amplitudes are then plotted in q space, and the phases are chosen so that a smooth curve would connect all the data points: we call this a phasing diagram (some subtle points were discussed in Torbet and Wilkins (1976) and Olah et al. (1991)). Examples of phasing diagram are shown in Figs. 2 and 3. If a phase transition takes place during dehydration, the data may separate into two distinct sets. For example, in Fig. 2 the data points for D = 49–47 Å form one set and D = 45–43 Å form another set. The data points in each set can be connected by a smooth curve (see Discussion).

With the phases determined, the relative scattering amplitudes are Fourier-transformed to obtain the scattering density profile ρ_{sc}. This profile is related to the true electron density ρ by $\rho = c\rho_{sc} + b$, with constants b and c. The presence of b is because the zero-order scattering amplitude is not measurable. These two constants can be determined if we know the composition of the sample, the molecular areas of the components normal to the bilayer, and the value of ρ at one point. We will use the electron density of the methyl group, 0.17 electrons/Å^3 (Nagle and Wilkinson, 1978) as the value of ρ at the center of the bilayer, ρ_0. Other input is as follows.

1) The number of electrons per molecule of DPhPC is 470.

2) The volume of DPhPC in the L_α phase is 1588 Å^3. This is estimated by $V_{DPhPC} = V_{DLPC} + 8V_{CH} + 8V_{CH_3}$, where the volume of 1,2-dilauroyl-*sn*-glycero-3-phosphatidylcholine (DLPC) is 992 Å^3 (Knoll, 1981), the volume of CH is 20.5 Å^3 (Tardieu et al., 1973), and the volume of CH_3 is 54 Å^3 (Nagle and Wilkinson, 1978). The volume of H_2O is 29.9 Å^3.

3) The smallest lamellar spacing during the swelling experiment of DPhPC was $D_{min} \approx 43$ Å at relative humidity about 50%. Previously, in an experiment with DLPC, we found by a gravitometric method that at 50% relative humidity DLPC contained 8% water by weight or three H_2O molecules per lipid (Olah, 1990). We assume that DPhPC also has three H_2O

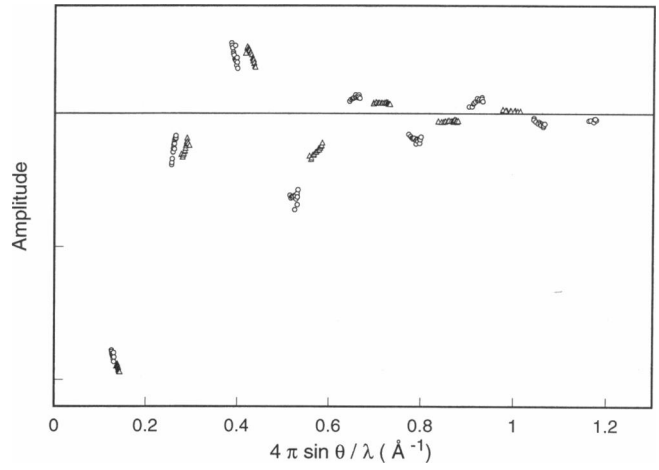

FIGURE 2 Phasing diagram for pure DPhPC. The data points clearly separate into two distinct sets (D > 47 Å (○) and D < 45.2 Å (△)). Each set can be connected by a smooth curve. This is clear evidence for a phase transition. Between the two sets, there is a gap in the D spacing. The multilayers of those D values were unstable, often separated into two coexistent phases (see Fig. 1, *middle*).

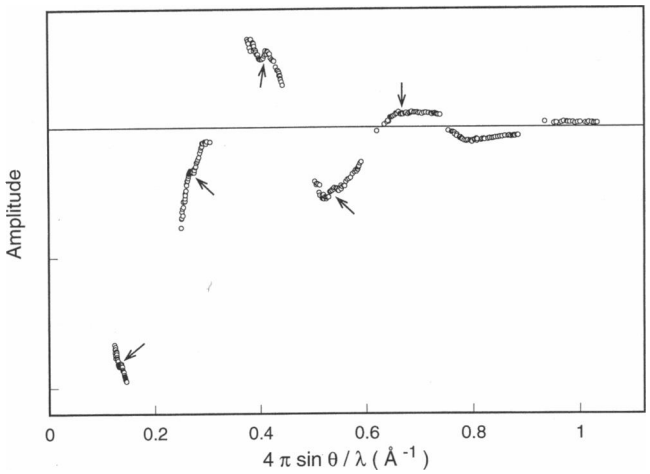

FIGURE 3 Phasing diagram for the alamethicin-DPhPC mixture at P/L = 1:47. The data points still separate into two distinct sets, indicating a phase transition (*arrows* show the points of discontinuity). Unlike pure DPhPC, which has a gap in the D spacing between the two phases, there are stable transitional states between the two phases here.

molecules associated with it under a similar condition. The cross section of DPhPC molecule is then approximately $\sigma = 2(1588 + 3\times29.9)\text{Å}^3/43\ \text{Å} = 76\ \text{Å}^2$. In comparison, the cross section of DLPC is estimated to be 52 Å^2 (Olah et al., 1991) and DPPC is estimated to be 62 Å^2 (Nagle, 1993).

4) Consider a unit cell of cross section σ consisting of two tail-to-tail DPhPC molecules and associated water, with a total length D. The total number of electrons in this unit cell is

$$n_e = 2x(\#\text{ of } e \text{ in DPhPC}) + 6x(\#\text{ of } e \text{ in } H_2O) + \frac{(D - D_{min})\sigma}{V_{H_2O}}(\#\text{ of } e \text{ in } H_2O).$$

which gives the total number of electrons per unit cross section of the bilayer

$$\frac{n_e}{\sigma} = 13.3 + 0.33(D - D_{min}).$$

The constants b and c are obtained from the two conditions

$$\int_D \rho dz = \frac{n_e}{\sigma}, \quad \text{and} \quad \rho(z = 0) = \rho_o,$$

where z is the coordinate normal to the plane of the bilayer. The sensitivity of our results to the choice of b and c will be discussed below.

For the samples containing a low concentration of alamethicin, $P/L \leq 1:47$, we added a fraction of alamethicin (electron number 1056) to the unit cell. The corrections to n_e are <2%.

RESULTS AND DISCUSSION

Bilayer thickness *t* versus lamellar spacing *D*

Figs. 4 and 5 show the normalized electron density profiles of pure DPhPC and DPhPC containing alamethicin. We define the bilayer thickness by the peak-to-peak distance of the profile, t, which corresponds to the phosphate-to-phosphate distance in the bilayer. This is a well defined length from the diffraction data, because the peak-to-peak distance is independent of the normalization for the electron density profile, or the choices of b and c. (The peak positions are defined by $d\rho(z)/dz = 0$, which is equivalent to $d\rho_{sc}(z)/dz = 0$.) In Fig. 6 we show t vs. D for the samples of pure DPhPC, P/L = 1:150, 1:80, and 1:47.

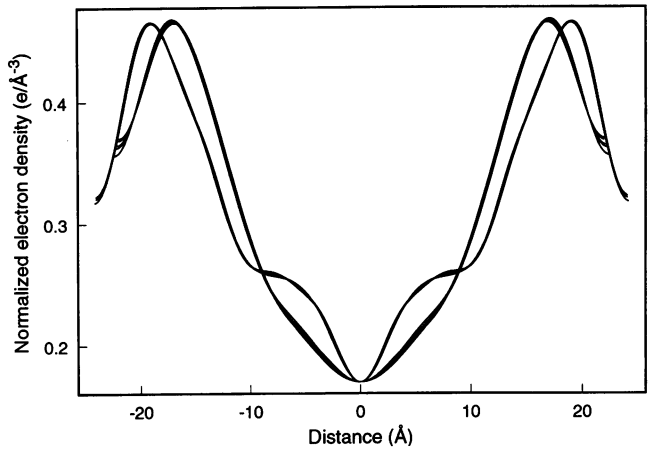

FIGURE 4 Normalized electron density profiles of pure DPhPC in the wet (D = 47.7–48.5 Å) and dry (D = 44.0–44.6 Å) phases. The width of the profile is D. The peak-to-peak distance is defined as the bilayer thickness t. t vs. D is shown in Fig. 6.

Water content and quality of diffraction pattern

We have found that phospholipids are more sensitive to humidity than most ordinary hygrometers, particularly near 100% relative humidity. For example, the D spacing of lipid multilayers can change as much as 1 Å from a slight change of humidity unmeasurable by commercial hygrometers. A change of the water content, if it takes place rapidly, may also affect the alignment of multilayers. The recovery time for a misaligned multilayer sample varies depending on the sample condition. In the preliminary stage of our experiment, the humidity was sometimes varied by too large a step. The

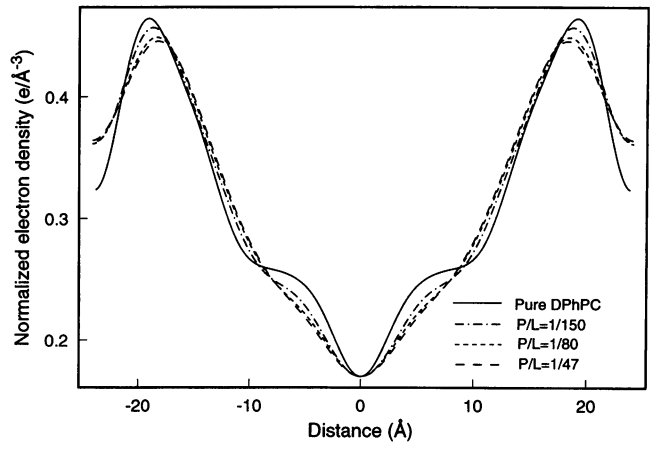

FIGURE 5 Normalized electron density profiles of the bilayers for P/L = 0 (D = 47.8 Å), P/L = 1:150 (D = 47.6 Å), P/L = 1:80 (D = 48.3 Å), and P/L = 1:47 (D = 48.2 Å). As the peptide concentration increases, the peak-to-peak distance decreases and the shoulders of the central trough progressively broaden, indicating an increasing degree of chain disorder.

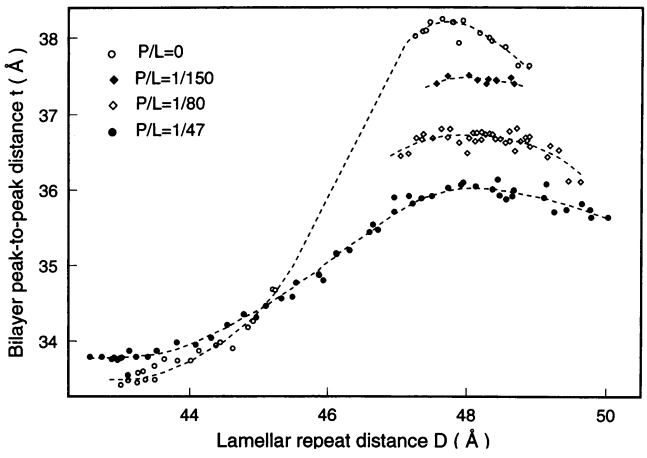

FIGURE 6 Bilayer thickness t vs. lamellar spacing D for pure DPhPC (P/L = 0), and for P/L = 1:150, 1:80, and 1:47. The points of highest D values were obtained at relative humidities between 95 and 100%. The points of lowest D values for P/L = 0 and 1:47 were obtained at relative humidities between 50 and 60%.

result was often a deterioration in the quality of the diffraction pattern, typically a substantial decrease in the overall diffraction intensities, broadening of the peaks, and loss of high Bragg orders. For example, the results of our preliminary experiments with P/L = 1:100 and 1:120 (not shown) were more scattered on the t vs. D diagram compared with the data shown in Fig. 6. This sudden deterioration of diffraction pattern with humidity change would not occur if the step of the humidity change were sufficiently small.

All samples (with or without alamethicin) with D > 47 Å exhibited apparent fluidity (the two substrates were fairly easily moved against each other). The presence of smectic defects seen under a polarized microscope showed that they were in the liquid crystalline state (Powers and Pershan, 1977; Asher and Pershan, 1979; Huang and Olah, 1987). At smaller D values (<46 Å), the samples appeared cloudy under the microscope, and it became difficult to move the two substrates against each other. As we will show below, a phase transition occurred between the wet (D > 47 Å) and the dry (D < 46 Å) conditions. For D < 44 Å, the rate of dehydration (as measured by the change in D) becomes exceedingly slow; therefore, we did not attempt to find the lowest possible D. The data shown in Fig. 6 were reproduced during the dehydration-hydration cycle, using at least two separate specimens.

The quality of the diffraction pattern, as measured by the number of discernible Bragg peaks, the widths of the peaks, and the overall diffraction intensities, is about the same for all of the data points presented in Fig. 6, although in general the overall intensities are somewhat higher in the dry region than in the wet region. The only exceptions are pure DPhPC in the wet region, where the eighth order and sometimes the ninth order are discernible. All of these features and the data in Fig. 6 have been reproduced independently by using multilayer samples on one substrate (i.e., without the Be plate) measured on a separate x-ray diffractometer, and essentially the same characteristics were exhibited by another amphiphilic helical peptide magainin (publication in preparation).

For D values greater than the values shown in Fig. 6, the quality of diffraction pattern slowly deteriorated with increasing D. (For D > ~53 Å, depending on the peptide concentration, the samples flowed on the vertical slide; therefore, they could not be measured.) We believe that the deterioration of the diffraction quality is due to the long range thermal undulations of the membranes, which become significant with increasing amount of water between bilayers (Caille, 1972; Nallet et al., 1993; Zhang et al., 1994). In the L_α phase, the apparent thickness t appears to increase slightly with decreasing D. The decrease of t for D < ~47.5 Å is due to a phase transition to be discussed below. Because the effect of thermal undulations may be larger at larger D, we will use the maximum values of t in the L_α phase for our quantitative analysis.

Because the quality of diffraction does affect the electron density profile and the parameters calculated from it, we stress the point that the data presented in Fig. 6 all have a comparable resolution. The fact that pure DPhPC in the wet region has one or two additional orders most likely is an intrinsic property of its bilayer form factor. There is no reason to believe that wet DPhPC is more ordered or has less thermal undulations than dry DPhPC. Also, the quality of diffraction did not change with peptide concentration, at least up to P/L = 1:47; if the difference between pure DPhPC and P/L = 1:150 were due to a change of resolution, one would expect the resolution to decrease progressively with the peptide concentration. As a rough measure of the effect of diffraction resolution on the electron density profile, a diffraction pattern of pure DPhPC containing nine orders was reanalyzed by excluding various numbers of high order peaks (Fig. 7). We see that the changes caused by excluding the eighth and ninth orders are small compared

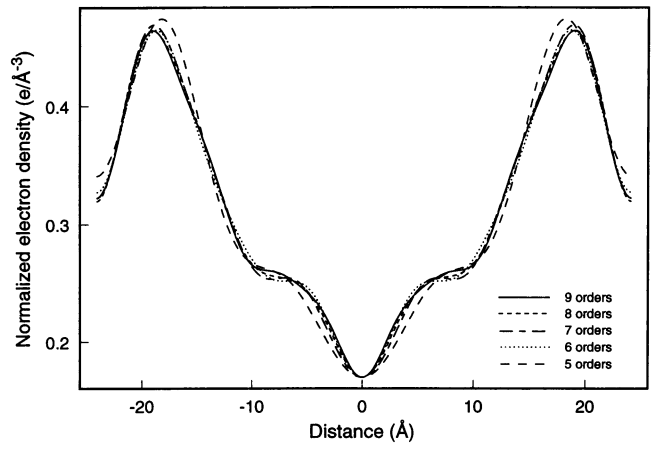

FIGURE 7 The effect of excluding high orders in a diffraction pattern. The diffraction pattern of pure DPhPC at D = 48.3 Å (shown in Fig. 1) has nine discernible Bragg orders. The electron density profiles of the first 5, 6, 7, and 8 orders are compared with the profile of 9 orders. Part of the 7-order and 8-order profiles cannot be distinguished from the 9-order profile. Note that appreciable broadening of the central trough (as compared with Fig. 5) does not occur until 4 orders are excluded.

with the changes produced either by dehydration (Fig. 4) or by alamethicin (Fig. 5). This demonstrates that the effect of any possible resolution differences between our diffraction patterns of different peptide concentrations is insignificant compared with the systematic changes by alamethicin shown in Figs. 5 and 6.

Finally, comparison of Fig. 6 with previous reports on the change of bilayer thickness with hydration should be made with caution. The earlier studies on this problem (e.g., Luzzati, 1968; Small, 1967; Lis et al., 1981) used a different method (Luzzati, 1968) to calculate the bilayer thickness (see McIntosh and Simon, 1986). Also, many of those examples were lipids in the gel phase where the hydrocarbon chains are tilted relative to the bilayer normal (e.g., DPPC in room temperature; Torbet and Wilkins, 1976). Within the L_α phase (D > 47 Å), we agree with McIntosh and Simon (1986) that the bilayer thickness is nearly unchanged with hydration.

Pure DPhPC

Diphytanoyl (3,7,11,15-tetramethylhexadecanoic) phosphatidylcholine is used often as a model membrane in the electrophysiological measurements, because it has long chains (16:0) while still in the liquid crystalline (L_α) phase in room temperature (Redwood et al., 1971). Most straight-chain lipids exhibit an order-disorder phase transition from a low temperature gel phase with close-packed, parallel chains in the all-*trans* state to a high temperature L_α phase where chains are no longer parallel, but include kinks and other similar conformations involving *trans-gauche* conformers. No L_α-to-gel phase transition was detected by differential thermal analyses for DPhPC in water over the temperature range from +120 to −120°C (Lindsey et al., 1979). This was attributed to the presence of methyl groups at regular intervals along the acyl chain, which causes the *trans* and one of the *gauche* rotamers to be nearly energetically equivalent and, moreover, the steric requirements of the methyl branches clearly prevent efficient lateral packing of the acyl chains.

It is rather surprising, therefore, that we detected a phase transition when DPhPC was dehydrated. The diffraction pattern in the middle of Fig. 1 shows double peaks in every Bragg order. The most common cause for such a pattern is inhomogeneity in the sample, i.e., two domains in different hydration states. In that case, one set of the peaks normally would disappear when the sample came to equilibrium. However, the double-peak pattern of pure DPhPC remained unchanged for days, indicating that two phases coexisted in equilibrium, which is an indication of a phase transition. Perhaps the clearest evidence for a phase transition is the phasing diagram Fig. 2. The data clearly split into two sets, one for each phase. There are no stable multilayers with D between ~45.2 and ~47 Å (Fig. 6). The wide-angle band near 9° is weak compared with those of straight-chains lipids like DLPC at ~10° (He et al., 1993; Fig. 1, *inset*). Unlike DLPC, whose wide-angle band becomes sharp upon dehydration (Fig. 1, *inset*), DPhPC has the same weak, diffuse band in the entire range of D, with and without alamethicin. The structural difference between the wet and dry phases of DPhPC is not known at this time.

1:150 ≤ *P/L* ≤ 1:47

We have reported previously (Huang and Wu, 1991) the OCD studies of alamethicin's insertion transition in a number of lipids. Alamethicin tends to insert perpendicularly into the bilayer at high concentrations and in high hydrations. If the system is dehydrated, the inserted peptide will move out of the bilayer and adsorb on the bilayer surface. On the other hand, below a critical concentration alamethicin adsorbs on the surface in all hydration conditions. This critical concentration depends on the lipid composition of the bilayer (Huang and Wu, 1991). Because we do not yet understand the principle of this lipid dependence, we were surprised to find that the critical concentration of alamethicin in DPhPC shifted from $P/L \sim 1{:}120$ in the previous experiment (Huang and Wu, 1991) to $P/L \sim 1{:}40$ in the current experiment. The cause of this change appeared to be a difference in the purity of Avanti's DPhPC, because the source of alamethicin remained the same (technical information from Sigma). The recent DPhPC from Avanti were made with chemically synthesized phytol. The purity of the final product is >99% in diacyl compounds and 97–98% phytanoyl (W. Shaw and S. Burgess, Avanti, personal communication). The DPhPC of the previous experiment (also from Avanti) was made with phytol isolated from pumpkin seeds; its purity was not clear.

The new critical concentration for insertion, $P/L \sim 1{:}40$, was reproduced consistently by many different sample preparation procedures. All samples for the x-ray experiment were examined first by OCD. At $P/L = 1{:}150$, 1:120, 1:100, 1:80, and 1:47, alamethicin was oriented parallel to the plane of the membrane in all hydration conditions. The results of the lamellar diffraction are shown in Figs. 5 and 6. We see in Fig. 6 that the gap in the D spacing of pure DPhPC is closed up in the case of $P/L = 1{:}47$, but the discontinuity in the phasing diagram due to the phase transition is still discernible (Fig. 3).

Interaction of DPhPC bilayers with alamethicin at low concentrations

The most striking feature of Fig. 6 is the systematic decrease of the bilayer thickness (in the L_α phase) with increasing peptide concentration. The electron density profiles (Fig. 5) show that the chain disorder increases (the central trough broadens) progressively with the peptide concentration. We interpret this with a simple physical picture. In a planar bilayer, the polar region and the hydrocarbon chain region of the lipid must maintain the same cross sectional area. In our case, the polar region consists of the phosphorylcholine groups and associated water molecules. All previous studies indicate that in pure lipid bilayers the phosphate and choline groups are, at same level, nearly parallel to the bilayer plane

(Worcester and Franks, 1976; Büldt et al., 1979). Suppose now that some peptide molecules are inserted in the polar region without displacing the water molecules out of the region or tilting the lipid headgroups out of the plane. Then the added cross sectional area in the polar region due to the adsorbed peptides must be matched by a corresponding areal increase in the chain region. In general, the cross sectional area of a lipid is larger if its chains are more disordered. Because the volume of the chains is constant, to the first order, during an order-disorder transition (e.g., the volume change at the gel-to-L_α phase transition is 4% for DPPC; Nagle and Wilkinson, 1978), the increase in the cross section is simply related to the decrease in the thickness of the chain region.

We now reverse the process and use the decrease in the bilayer thickness to calculate the chain-area expansion per lipid: $\Delta A = (d_0 - d)(A_0/d_0)$, where A_0 is the cross section of a DPhPC in the pure lipid bilayer and d_0 is the corresponding thickness of the chain region; d is the thickness of the chain region when the peptide to lipid molar ratio is P/L (Fig. 8). d is estimated from the bilayer thickness t by $t/2 = d + 4.0$ Å, where the distance from the phosphate to the chain region is estimated to be about 4.0 Å. (estimated from a minimum free energy molecular model. It should be stressed that a change of this distance by a few Å would not change the main conclusion below.) d_0 is obtained from t_0 in Fig. 6 to be 15.1 Å. A_0 was estimated previously to be 76 Å^2 (see Materials and Methods).

The quantity $\Delta S = \Delta A(L/P)$ is then the expanded area for each adsorbed peptide molecule. Defining the t values (38.2, 37.5, 36.7, and 36.0 Å) as the maxima of the curves fitted to the data in Fig. 6 for P/L = 0, 1:150, 1:80, and 1:47 and, similarly (37.2 and 37.0 Å) to the data of P/L = 1:120 and 1:100 (not shown), we found that ΔS is a constant ~280 ± 20 Å^2. (If ΔS is a constant, $(d_0 - d)$ is proportional to P/L; this is shown in Fig. 9 with our estimated maximum error bars.) This value is close to the estimated lengthwise cross section of alamethicin. From the unit cell of alamethicin crystal (space group $P2_1$, a = 33.33, b = 29.62, c = 23.20 Å, β = 120.4°, Z = 6; Fox and Richards, 1982), we estimate the lengthwise cross section of alamethicin to be ~350 Å^2 (if the molecule is a right circular cylinder, the diameter of the circular cross section is 11 Å and the cross section through the axis is 370 Å^2; if it is a square cylinder, the sides of the square are 10 Å and the area of the long side is 330 Å^2). Thus, the most reasonable conclusion is that alamethicin resides within the polar region (which is ~10 Å thick based on space-filling models), adsorbs at the interface of the chain region, and separates the lipid headgroups laterally to create an additional area of about 280 Å^2 in the polar region. The discrepancy of 70 Å^2 between the 280 and the 350 Å^2 implies one or a combination of the following three possibilities. 1) Each peptide adsorption displaces about seven water molecules from the polar region. 2) If a phosphorylcholine headgroup is tilted from the parallel to the perpendicular orientation relative to the plane of bilayer, an area of about 25 Å^2 will be created. Thus, three tilted headgroups could account for the 70 Å^2 discrepancy. 3) The crystals of alamethicin contained 30% solvent, similar to that found for small globular proteins grown from aqueous solvents (Fox and Richards, 1982). If we exclude the solvent from the volume of alamethicin, the estimated cross section for alamethicin would decrease by 20%, making it ~280 Å^2. In that case, there is no significant discrepancy between the expanded area and the peptide cross section. In all cases, it appears that alamethicin is inserted in the polar region with minimal disturbance to the headgroups and their associated water molecules.

What is amazing is that the entire bilayer is compressed by such a low concentration of peptide. Consider the sample

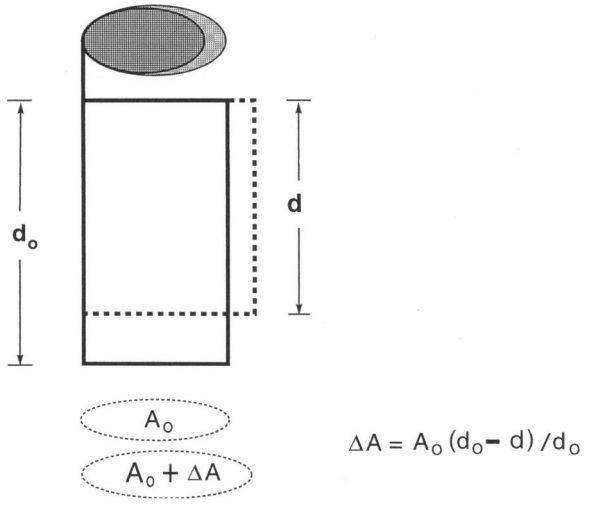

FIGURE 8 A lipid molecule in a planar bilayer. The polar region consisting of the phosphorylcholine headgroup (*shaded dark*) and its associated water (*shaded light*) has the same cross sectional area as the chain region (*filled rectangle*). The volume of the chains is constant, to the first order, during an order-disorder transition. Therefore, the decrease in the thickness of the chain region $(d_0 - d)$ is proportional to the increase in the cross sectional area ΔA.

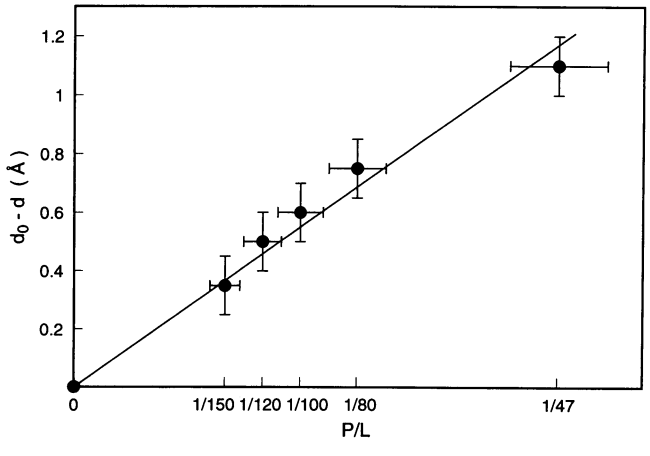

FIGURE 9 The decrease in the thickness of the chain region $(d_0 - d) = (t_0 - t)/2$ is proportional to the peptide concentration P/L. The error bars represent our estimated maximum errors: 10% in P/L allowing variations in the impurity of peptide and lipid from different sample lots; ±0.1 Å in $(d_0 - d)$ representing the statistical errors of curve fittings to the data points in Fig. 6. The straight line is a line of constant proportion.

of $P/L = 1{:}150$. If the peptide molecules are distributed uniformly on the membrane surface, the distance between two peptide molecules is ~120 Å. Because the entire bilayer is compressed (Fig. 5), it implies that each (or most) of all 150 lipids is shortened and contributes to the creation of the additional area for one peptide. This is contrary to a model in which the bilayer perturbation by a peptide is assumed to be local. In the latter case, one would expect that the overall bilayer thickness remains essentially the same as the pure lipid, when the peptide concentration is as low as 1:150. Thus, a lipid bilayer tends to spread a deformation over a large area, as much as 100 Å in diameter, rather than dimple locally. This long range nature of bilayer deformation is due to a splay term in the elastic free energy (Huang, 1986). (The splay term is similar to the bending energy, proportional to the square of the curvature of the interface (Helfrich, 1973). We use the liquid-crystal terminology because splay seems more suitable to describe the deformation of a bilayer with a finite thickness, where we treat the two hydrophilic-hydrophobic interfaces separately. Helfrich's term usually describes the bending of the bilayer as a mathematical surface, i.e., without thickness.) Many membrane theories assume that a bilayer deformation decays exponentially in distance along the plane of the bilayer, essentially ignoring the splay term (e.g., the theories reviewed in Abney and Owicki, 1985; Sperotto and Mouritsen, 1991). Qualitatively, the inclusion of the splay term in the free energy makes the bilayer deformation profile basin-like (Fig. 10 *A*), because the profile has a concave-convex inflection that extends the range of deformation. Without the splay term, the deformation profile essentially follows an exponential curve (Fig. 10 *B*).

Thus, the physical picture of the peptide-membrane interaction at low concentrations is as follows. A majority of the peptide molecules are adsorbed at the interfacial region of the bilayer with the helical axes parallel to the plane of the interface. The adsorbing peptide pushes the lipid headgroups laterally to create the space. The relatively uniform bilayer compression observed at low peptide concentrations is consistent with a dispersed (rather than an aggregated) distribution of the adsorbed molecules. Probably a very small fraction of the peptide molecules are inserted, in equilibrium partition, in the bilayer. This fraction may increase if there is a transmembrane electric potential because helical peptides possess a dipole (Wada, 1976; Huang and Wu, 1991). Presumably, the inserted peptide molecules form ion channels as detected in conduction measurements (e.g., Latorre and Alvarez, 1981; Opsahl and Webb, 1994). As the peptide concentration increases, the thickness of the chain region decreases in proportion. Because the bilayer deformation free energy increases quadratically with the thickness compression (Huang, 1986), it increases quadratically with the peptide concentration. The critical concentration for insertion is reached when the energy of adsorption per peptide, which includes the energy of binding to the interface and the energy of membrane deformation, becomes equal to the energy of insertion (publication in preparation).

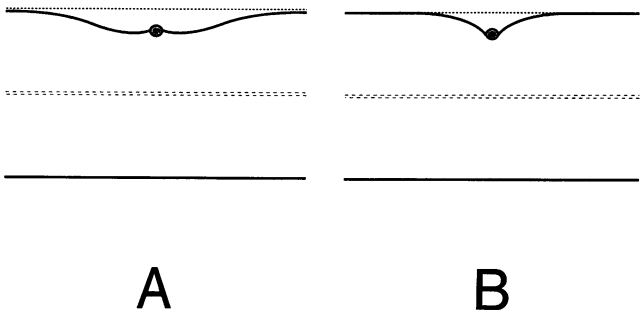

FIGURE 10 Schematic profile of a monolayer interface (the hydrophobic-hydrophilic interface) when an amphiphilic peptide (*circle*) is adsorbed. The single dotted line is the unperturbed interface; the double dotted lines represent the median plane of the bilayer. The opposite monolayer is assumed to be unperturbed. (*A*) Schematic deformation profile calculated from a free energy including the splay term (the exact mathematical form is given in Huang, 1986). (*B*) Schematic deformation profile calculated from a free energy without the splay term — the deformation decays exponentially.

We thank J. F. Nagle for discussions, particularly on the hydration problem. This research was supported in part by National Institutes of Health grant AI34367 and Biophysics Training grant GM08280, Department of Energy grant DE-FG03–93ER61565, and by the Robert A. Welch Foundation.

REFERENCES

Abney, J. R., and J. C. Owicki. 1985. Theories of protein-lipid and protein-protein interactions in membranes. *In* Progress in protein-lipid Interactions. A. Watts and J. De Pont, editors. Elsevier, New York.

Asher, S. A., and P. S. Pershan. 1979. Alignment and defect structures in oriented phosphatidylcholine multilayers. *Biophys. J.* 27:137–152.

Blaurock, A. E. 1971. Structure of the nerve myelin membrane: proof of the low resolution profile. *J. Mol. Biol.* 56:35–52.

Büldt, G., H. U. Gally, J. Seelig, and G. Zaccai. 1979. Neutron diffraction studies of phosphatidylcholine model membranes. I. Head group conformation. *J. Mol. Biol.* 134:673–691.

Caille, A. 1972. Remarques sur la diffusion des rayons X dans les smectiques. *C. R. Acad. Sci. Series B.* 274:891–893.

Chang, D. T., C.-S. C. Wu, and J. T. Yang. 1978. Circular dichroic analysis of protein conformation: inclusion of the β-turns. *Anal. Biochem.* 91: 13–31.

Fox, R. O., and F. M. Richards. 1982. A voltage-gated ion channel model inferred from the crystal structure of alamethicin at 1.5-Å resolution. *Nature.* 300:325–330.

Gibson, B. W., D. Tang, R. Mandrell, M. Kelly, and E. R. Spindel. 1991. Bombinin-like peptides with antimicrobial activity from skin secretions of the Asian toad, *Bombina orientalis*. *J. Biol. Chem.* 266:23103–23111.

Habermann, E. 1972. Bee and wasp venoms. *Science.* 177:314–322.

He, K., S. J. Ludtke, Y. Wu, and H. W. Huang. 1993. X-ray scattering with momentum transfer in the plane of membrane: application to gramicidin organization. *Biophys. J.* 64:157–162.

Helfrich, W. 1973. Elastic properties of lipid bilayers: theory and possible experiment. *Z. Naturforsch.* 28C:693–703.

Huang, H. W. 1986. Deformation free energy of bilayer membrane and its effect on gramicidin channel lifetime. *Biophys. J.* 50:1061–1070.

Huang, H. W., and G. A. Olah. 1987. Uniformly oriented gramicidin channels embedded in thick monodomain lecithin multilayers. *Biophys. J.* 51:989–992.

Huang, H. W., W. Liu, G. A. Olah, and Y. Wu. 1991. Physical techniques of membrane studies: study of membrane active peptides in bilayers. *Progr. Surf. Sci.* 38:145–199.

Huang, H. W., and Y. Wu. 1991. Lipid-alamethicin interactions influence alamethicin orientation. *Biophys. J.* 60:1079–1087.

Kaiser, E. T., and F. J. Kézdy. 1987. Peptides with affinity for membranes. *Annu. Rev. Biophys. Chem.* 16:561–581.

Knoll, W. 1981. Volume determination of deuterated dimyristoyllecithin by mass and scattering length densitometry. *Chem. Phys. Lipids*. 28:337–345.

Latorre, R., and S. Alvarez. 1981. Voltage-dependent channels in planar lipid bilayer membranes. *Physiol. Rev.* 61:77–150.

Lee, J. Y., A. Boman, S. Chuanxin, M, Andersson, H. Jornvall, V. Mutt, and H. G. Boman. 1989. Antibacterial peptides form pig intestine: isolation of a mammalian cecropin. *Proc. Natl. Acad. Sci. USA*. 86:9159–9162.

Lindsey, H., N. O. Petersen, and S. I. Chan. 1979. Physicochemical characterization of 1,2-diphytanoyl-*sn*-glydero-3-phosphocholine in model membrane systems. *Biochim. Biophys. Acta.* 555:147–167.

Lis, L. J., W. T. Lis, V. A. Parsegian, and R. P. Rand. 1981. Adsorption of divalent cations to a variety of phosphatidylcholine bilayers. *Biochemistry*. 20:1771–1777.

Ludtke, S. J., K. He, Y. Wu, and H. W. Huang. 1994. Cooperative membrane insertion of magainin correlated with its cytolytic activity. *Biochim. Biophys. Acta.* 1190:181–184.

Luzzati, V. 1968. X-ray diffraction studies of lipid-water systems. *In* Biological Membranes. D. Chapman, editor. Academic Press, New York. 71–123.

McIntosh, T. J., and S. A. Simon. 1986. Hydration force and bilayer deformation: a reevaluation. *Biochemistry*. 25:4058–4066.

Moffitt, W. 1956. Optical rotatory dispersion of helical polymers. *J. Chem. Phys.* 25:467–478.

Nagle, J. F. 1993. Area/lipid of bilayers from NMR. *Biophys. J.* 64:1476–1481.

Nagle, J. F., and D. A. Wilkinson. 1978. Lecithin bilayers: density measurements and molecular interactions. *Biophys. J.* 23:159–175.

Nallet, F., R. Laversanne, and D. Roux. 1993. Modelling x-ray or neutron scattering spectra of lyotropic lamellar phases: interplay between form and structure factors. *J. Phys. II France*. 3:487–502.

O'Brien, F. E. M. 1948. The control of humidity by saturated salt solutions *J. Sci. Instrum.* 25:73–76.

Olah, G. A. 1990. Tl^+ distribution in the gramicidin ion channel determined by x-ray diffraction. Ph.D. thesis. Rice University, Houston, TX. 82 pp.

Olah, G. A., and H. W. Huang. 1988. Circular dichroism of oriented α helices. I. Proof of the exciton theory. *J. Chem. Phys.* 89:2531–2537.

Olah, G. A., H. W. Huang, W. Liu, and Y. Wu. 1991. Location of ion binding sites in the gramicidin channel by x-ray diffraction. *J. Mol. Biol.* 218: 847–858.

Opsahl, L. R., and W. W. Webb. 1994. Transduction of membrane tension by the ion channel alamethicin. *Biophys. J.* 66:71–74.

Pandey, R. C., J. C. Cook, and K. L. Rinehart. 1977. High resolution and field desorption mass spectrometry studies and revised structure of alamethicin I and II. *J. Am. Chem. Soc.* 99:8469–8483.

Powers, L., and P. S. Pershan. 1977. Monodomain samples dipalmitoylphosphatidylcholine with varying concentrations of water and other ingredients. *Biophys. J.* 20:137–152.

Redwood, W. R., F. R. Pfeiffer, J. A. Weisbach, and T. E. Thompson. 1971. Physical properties of bilayer membranes formed from a synthetic saturated phospholipid in n-decane. *Biochim. Biophys. Acta.* 233:1–6.

Saxena, A. M., and B. P. Schoenborn. 1977. Correction factors for neutron diffraction from lamellar structures. *Acta. Cryst.* A33:813–818.

Segrest, J. P., H. De Loof, J. G. Dohlman, C. G. Brouillette, and G. M. Anantharamaiah. 1990. Amphipathic helix motif: class and properties. *Proteins*. 8:103–117.

Small, D. M. 1967. Phase equilibria and structure of dry and hydrated egg lecithin. *J. Lipid Res.* 8:551–557.

Sperotto, M. M., and O. G. Mouritsen. 1991. Monte Carlo simulation studies of lipid order parameter profiles near integral membrane proteins. *Biophys. J.* 59:261–270.

Steiner, H., D. Hultmark, A. Engström, H. Bennich, and H. G. Boman. 1981. Sequence and specificity of two antibacterial proteins involved in insect immunity. *Nature*. 292:246–248.

Tardieu, A., V. Luzzati, and F. C. Reman. 1973. Structure and polymorphism of the hydrocarbon chains of lipids: a study of lecithin-water phases. *J. Mol. Biol.* 75:711–733.

Torbet, J., and M. H. F. Wilkins. 1976. X-ray diffraction studies of lecithin bilayers *J. Theor. Biol.* 62:447–458.

Wada, A. 1976. The α-helix as an electric macro-dipole. *Adv. Biophys.* 9:1–63.

White, J. M. 1992. Membrane fusion. *Science*. 258:917–924.

Worcester, D. L., and N. P. Franks. 1976. Structural analysis of hydrated egg lecithin and cholesterol bilayers. II. Neutron diffraction. *J. Mol. Biol.* 100:359–378.

Wu, Y., H. W. Huang, and G. A. Olah. 1990. Method of Oriented Circular Dichroism. *Biophys. J.* 57:797–806.

Zasloff, M. 1987. Magainins, a class of antimicrobial peptides form *Xenopus* skin: isolation, characterization of two active forms and partial cDNA sequence of a precursor. *Proc. Natl. Acad. Sci. USA*. 84:5449–5453.

Zhang, R., R. M. Suter, and J. F. Nagle. 1994. Theory of the structure factor of lipid bilayers. *Phys. Rev.* E50:5047–5060.